IMT – INSTITUT DE MICROTECHNIQUE

LABORATOIRE DE PRODUCTION MICROTECHNIQUE (LPM)

Caroline JACQ
CH-1015 LAUSANNE, Switzerland
☎: + 41 21 693 53 85
Fax : + 41 21 693 38 91
Caroline.jacq@epfl.ch
http://lpm.epfl.ch

ÉCOLE POLYTECHNIQUE
FÉDÉRALE DE LAUSANNE

CO-ME II-6-3 final report

Load sensing surgical instruments

Development and characterisation of low firing thick-film materials systems for medical steels

Caroline Jacq, Thomas Maeder & Peter Ryser, 19.1.2010
Laboratoire de Production Microtechnique (LPM)
École Polytechnique Fédérale de Lausanne
EPFL, Station 17, CH-1015 Lausanne, http://lpm.epfl.ch/tf

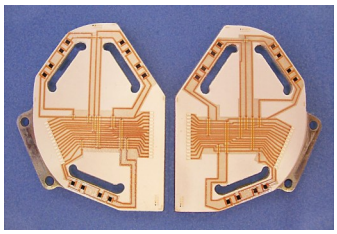

Summary

The goal of this project was to develop low-firing thick-film materials systems for the fabrication of piezoresistive sensors on special steels, for the fabrication of instrumented medical devices. To this end, a series of individual thick-film materials and complete systems, based on lead borosilicate glasses, were developed and extensively characterised. These studies allowed us to formulate an optimised system firing at 625°C and applicable to austenitic, ferritic and martensitic steels. The functionality of this system was demonstrated with several steels by manufacturing pressure sensors and – in this report – by successfully instrumenting the previously developed knee-balancing force sensor [1].

The moderate achieved firing temperature strongly reduces compatibility problems with steels, compared to standard thick-film systems that require firing at 850°C: oxidation and annealing of the steel are considerably reduced, and, especially, phase transition problems are eliminated, allowing the use of high-strength martensitic steels as substrates.

Finally, preliminary studies were carried out to eliminate lead from our materials, by replacing lead borosilicate glasses by compositions in the bismuth-zinc borosilicate system, with successful proof-of-principle results.

Table of contents

1. Introduction

1.1. Load sensing in surgical instruments & implants

The overall object of this project is the application of force and pressure sensing technology to smart surgical instruments as well as implants. Smart instruments allowing direct feedback of loads to the surgeon lead to better reliability and success of surgical operations such as total knee arthroplasty (TKA, Figure 1). Load-sensing implants may also be a useful tool in monitoring patient recovery in cases such as bone fracture and in aiding the re-education process.

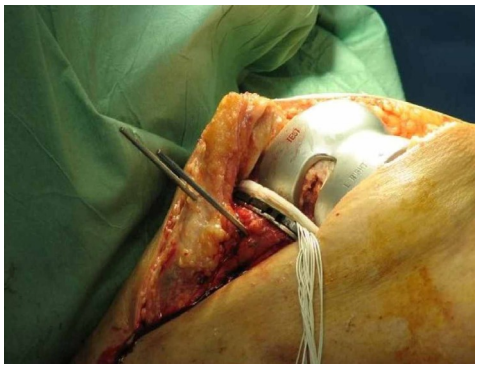

Figure 1: Using smart surgical instrument for TKA [1].

Recent studies [2][3] have shown that two common causes of complications after TKA (Figure 2) are due to loosening and instability due to misalignment and ligamentous imbalance. While misalignment may be efficiently corrected by modern navigation systems, the surgeon balances up to now the collateral knee joint ligaments by “hand”. Based on his feeling and perception, the surgeon manipulates the knee joint in order to ensure the optimal balance needed for a stable artificial joint. However, this "manual" procedure is subjective, and leads to relatively large errors that can cause pain and premature wear of the implant. Therefore, the innovative demonstrator for this project, depicted in Figure 3, is a force-sensing device to intraoperatively measure knee joint forces and moments for optimal ligament balancing during a total knee arthroplasty, developed in a previous phase of CO-ME [1][4][5][6][7]. The sensor is composed of two sensitive parts, one for each condyle (Figure 4), covered by thick-film piezoresistive sensors.

Figure 2: Knee joint before and after TKA [8].

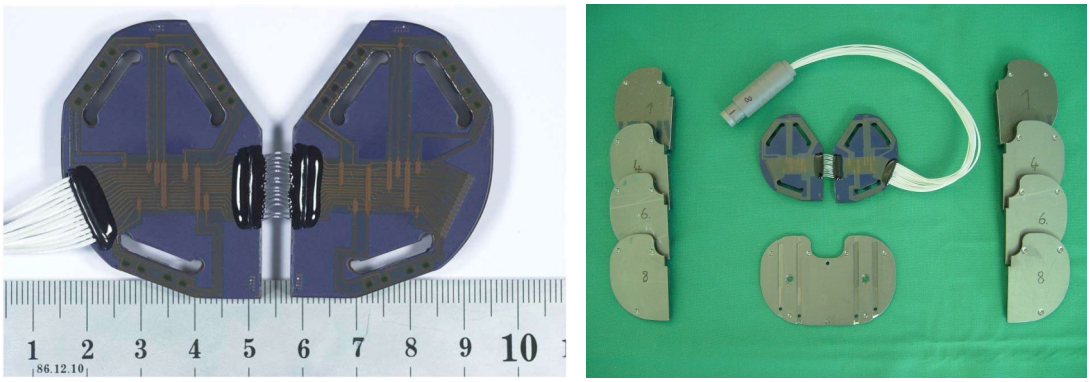

Figure 3: Force sensor for TKA (left) [1] with sets of wedges (right).

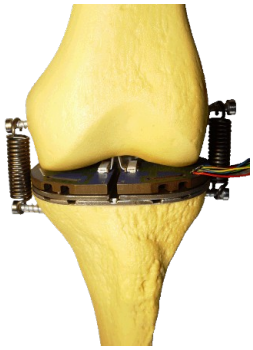

Figure 4: Force sensor in knee joint [1].

1.2. Materials issues

A well-established, low production cost solution for force and pressure sensing is thick-film piezoresistive technology [9][10][11][12], usually applied on ceramic alumina substrates. This technology features good temperature and chemical stability, which is necessary to withstand sterilisation cycles. However, alumina is not optimal for piezoresistive sensing applications, as it is brittle, its elastic modulus high and its strength rather low. Stronger ceramics such as zirconia and zirconia-toughened alumina (ZTA) exist, but, being brittle, their strength is easily degraded by processing-induced defects [13], which include the presence of the thick-film sensing layers [14][15]. These issues can be avoided by using metallic substrate materials such as high-strength stainless steels and Ti alloys [16], which are commonly applied for medical instruments, fixtures and implants.

In a first step, fabrication of the ligament-balancing sensor was attempted using commercial thick-film systems with a standard firing temperature (850°C). However, these firing conditions are not compatible with Ti alloys, which oxidise too extensively. Moreover stainless steels undergo degradation of mechanical properties due to annealing or phase transformations incompatible with the presence of thick-film layers. Better strength was attained with a special austenitic stainless steel grade with solution strengthening by nitrogen additions, such as the alloy used for the TKA sensor, Sandvik Bioline High-N [17]. However, this steel is very expensive to machine. Another issue was its very high coefficient of thermal expansion (CTE), ca. 17 ppm/K (vs. 11 for ferritic / martensitic steels and 7 for alumina, the standard thick-film substrate). This high CTE forced, even in this first version, the partial introduction of low-firing thick-film compositions (for crossovers) in order to avoid excessive stresses and allow production of a first series of sensors. Use of a fully commercial system was not possible; upon firing of the crossover dielectric, spallation tended to occur, as

depicted in Figure 5, due to the high compressive stresses in the dielectrics. As this occurred mainly on zones having buried conductors, it is thought the dielectric-conductor-dielectric edges (see figure) acted as crack initiation points, by stress concentration. This problem was essentially solved by using a low-stress crossover dielectric formulated with a low-melting glass. However, yield and reliability were still somewhat problematic due to the high compressive stresses in the main dielectric.

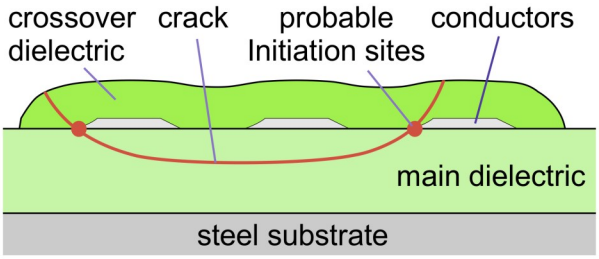

Figure 5. Schematic depiction of spalling failures occurring with standard dielectrics & crossovers.

1.3. Subject of this report

In order to solve these problems and allow the use of high-strength (and lower CTE) Ti alloys or martensitic steels, we endeavoured to develop thick-film materials systems featuring low firing temperature (<650°C) [18][19][20][21][22][23][24][25][26]. The first goal was to develop such a system with high reliability, especially good adhesion on the metal substrate and good stability, and compatibility to both ferritic / martensitic and austenitic steels. A typical piezoresistive thick-film materials sequence is schematised on Figure 6. Such a system mainly comprises dielectric, conductor and resistor materials, with the optional addition of an "overglaze" glassy protection layer, and must meet the following requirements:

- Compatibility of the coefficients of thermal expansion (CTE) between the metallic substrate and the thick-film multilayer
- Good chemical adherence of the dielectric on the metallic substrate
- Chemical compatibility between the dielectric and conductor / resistor layers – low and "normal" termination effects [27][28]
- Good strain-sensing properties
- Reliability: low process sensitivity, good reproducibility and good long-term stability

This report reviews the development of this first-generation low-firing system and details its application to the ligament-balancing knee sensor [1][4][6], compared to the previously-used mainly commercial thick-film materials system Finally, first pomising results [28][29] for new lead-free thick-film materials are presented.

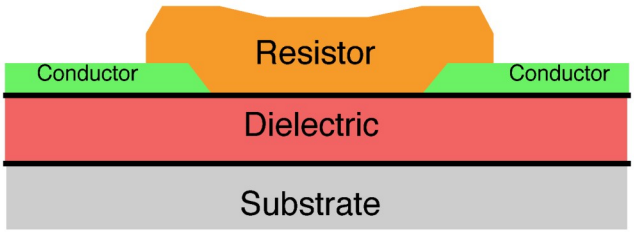

Figure 6: Schematic cross-section of thick-film sequence on the substrate (thicknesses not to scale & optional overglaze not shown).

2. Development of a low-firing thick-film materials system

2.1. Overview

Given the aforementioned requirements, it appears rapidly that the dielectric is by far the most critical material (Figure 6 & Figure 7).

- It makes chemical contact with all the other layers.
- It is responsible for the critical mechanical bonding to the steel.
- It is by far the most voluminous material, with a thickness of ca. 50…150 µm (depending on the required electrical insulation), compared to ca. 10…20 µm for the resistor, and covering the entire circuit surface. Therefore CTE matching to the substrate mainly concerns the dielectric.
- No appropriate commercial materials exist, the closest being some specialised compositions for aluminium substrates with limited applications [30].

The situation for conductors and resistors is less critical. Commercial conductor and resistor materials do exist for firing at ca. 600°C [25][26]. Moreover, CTE matching is much less important, given the small resistor volumes and the ductile nature of the conductors.

Measuring bridge	Conductor & resistor layers (+ overglaze)
Dielectric 3 : compatibility	Chemical compatibility with conductors & resistors
Dielectric 2 : main layer	Good CTE matching Electrical insulation Refire stability (no re-melting)
Dielectric 1 : adhesion	Adhesion promoters + good CTE matching
Substrate	Medical alloy – steel

Figure 7: Thick-film layer sequence on metal, detailing the different functions of the dielectric.

2.2. Glasses

Except commercial compositions, all formulations we developed in this study are based on the same two glasses, which were developed for both our loaded-glass type dielectrics [31] and our studies on low-firing resistors [18][20][23][25][26][32][33][34][35][36]. They are based on the lead borosilicate system [37][38], as are glasses for standard thick-film resistors, with an increased PbO content to obtain lower processing temperatures and an extra 2% Al_2O_3 added to suppress crystallisation [39]. Their data is given in Table 1.

For dielectrics or resistors, the ideal firing temperature lies ca. 100°C above the densification temperature of the glass alone, namely around 600°C for V6-based materials and around 500°C for V8-based ones. In this study, all dielectrics and self-formulated resistors [34][36] base on V6. Lower-melting V8 was used to formulate fritted conductors and overglaze compositions.

Dielectric	**V6**	**V8**	
PbO	75	85	[%mass]
B_2O_3	10	10	[%mass]
SiO_2	15	5	[%mass]
Al_2O_3	2	2	[%mass]
Densification temperature	500	400	[°C]
CTE	9.0	10.5	[ppm/K]

Table 1. Composition of both glasses.
Percentages refer to $PbO+B_2O_3+SiO_2$. CTE from [38].
Approximate densification temperature for 10 min at peak.

2.3. Low-firing thick-film dielectrics

The many requirements for the dielectric layer may be partially conflicting and therefore problematic to fulfil with a single material. For instance, additives to improve adhesion and CTE matching may harm chemical compatibility with the resistor or even the insulating properties of the dielectric. However, these different functions may be carried out by different layers, as illustrated in Figure 7.

- The 1st composition insures good adhesion. CTE matching is important for this layer, but can be made less critical if need be by keeping the thickness moderate.
- The 2nd composition is mainly responsible for the electrical insulation and CTE matching. Another very important function here is refire stability; it must provide a sound mechanical basis for the overlying layers, without excessive remelting.
- The 3rd dielectric composition is responsible for chemical compatibility. Often, this is only needed for the resistor.

Adhesion layer

Preliminary studies showed poor adhesion of standard dielectrics to stainless steels, a situation only somewhat improved by prior oxidation of the substrate. This is thought to be due to the peculiar reactions between Cr_2O_3 (dominant oxide scale on the steel) and the PbO in the glass [40][41], where Cr changes valence from +3 to +6:

$$4PbO + 2Cr_2O_3 + 3O_2 \rightarrow 4PbCrO_4 \quad (1)$$

This, together with the oxygen depletion brought about by oxidation of the steel, may locally initiate reduction of PbO in the glass to metallic Pb. Therefore, to provide a source of oxygen and thereby insure a good adhesion, the first dielectric layer was filled with Fe_2O_3, which provides a source of oxygen by partial reduction of Fe^{3+} to Fe^{2+} without major disturbances in the glass. While we did not confirm its supposed mode of action, Fe_2O_3 was indeed found to be an efficient adhesion promoter for dielectric on steel, failure nearly never occurring at the metal-dielectric interface [26].

Main layer - CTE adjustment

In order to address to the thermal expansion issue, the CTE of this layer was adjusted by adding suitable fillers to the glass matrix, according to the metallic substrate, which provide mechanical stabilisation of the dielectric as well. This "main" dielectric composition was used for crossover dielectric as well.

For the ferritic and martensitic stainless steels, which have a CTE of ~11ppm/K, we used quartz, and, for the austenitic stainless steels, which have a higher CTE of ~17 ppm/K, cristobalite. In the temperature interval between 25 and 500°C, quartz and cristobalite have an average CTE of ca. 17 and 40 ppm/K respectively [42]. For cristobalite, this exceptionally high average thermal expansion is due to a phase transition occurring around 260°C. Quartz has a phase transition at a higher temperature, 575°C, that nevertheless adds non-linearity of its thermal expansion curve below that temperature.

While the high degree of filler loading might lead us to expect an excessive CTE, dissolution of SiO_2 into the glass [20][21] reduces this effect, and therefore must be accounted for. Dissolution reduces CTE in two ways: 1) the amount of high-CTE filler decreases, and 2) SiO_2 enrichment of the glass lowers its CTE as well. Ideally, using powders coated with an inert diffusion barrier (Al_2O_3, for instance) could both minimise these problems and improve chemical compatibility with the resistor (see below).

Chemical compatibility layer

The aforementioned partial dissolution of the silica fillers into the high-lead V6 glass lead to poor compatibility with V6-based resistors, or with the commercial composition ESL 3114 [43], which is thought to be based on a similar glass – its nominal firing temperature is 625°C, and its materials safety data sheet (MSDS) states its glass contains lead, with – one slight difference with our glasses – some additional cadmium. SiO_2 added to the glass has in fact been shown to lead to strong increases in resistance values and decreases of the temperature coefficient of resistance (TCR) [44].

Therefore, a chemical compatibility layer is required [26]. This dielectric was filled with alumina powder, which has poor CTE matching to the steel, but is more inert towards the resistor.

Dielectric multilayer build-up & concluding remarks

The overall thickness of the dielectric is ca. 100 µm, and it is built up of 4 separately printed and fired layers (Table 2), as stated in the corresponding studies [25][26]. While breakdown strength was not tested here, good results have been measured with similar dielectrics based on V6 glass [18][19].

Overall, the dielectrics in this system essentially essentially belong to the so-called unreactive filled dielectric type, which is not the most favourable option, as it entails a necessary compromise between densification ability and refire stability [45][46]. Therefore, crystallisable dielectrics are preferred, or, alternatively, reactive ones where part of the glass reacts with the filler [47][48]. We were successful in formulating such a composition [22], but the resulting very low thermal expansion, due to PbO depletion of the glass [38] and $PbTiO_3$ formation [49]. Reactive dielectrics with higher CTE values could in principle be obtained by using fillers such as MoO_3, which yields $PbMoO_4$ [47][50].

Layer (# prints)	**Thickness** [µm]	**Glass** [%vol.]	**Filler** [%vol.]
Crossover (2x)	20	(= main)	(= main)
Compatibility (1x)	20	50 V6	50 Al_2O_3[1]
Main (2x)	60	40 V6	60 SiO_2†
Adhesion (1x)	20	75 V6	25 Fe_2O_3[2]

Table 2. Dielectric multilayer buildup (all layers fired at 625°C).
† SiO_2 : cristobalite[3] for austenitic steels (here) or quartz[4] for ferritic / martensitic ones.

2.4. Other layers

Conductor, crossover dielectric and resistor deposition

As for the dielectric, deposition of conductors and resistor layers followed the optimised scheme developed in our previous study [26].

- First, the solder pads and main conductive tracks are deposited and dried (not fired) using a layer of commercial ESL 9912 Ag conductor. ESL 9912 gives good adhesion and solderability, but, pre-fired on dielectric, it does not constitute a good termination. Therefore, this layer does not comprise the resistor terminations.
- Then, the commercial resistors ESL 3114 (10 kΩ) is printed and co-fired with the 1st conductor at 625°C and 1st crossover dielectric layer.
- The 2nd crossover dielectric layer is printed and fired at 625°C.
- Finally, a custom conductor consisting of Ag powder[5] (90% vol.) and V8 glass (10% vol.) acting as a low-melting frit was printed and post-fired at 500°C. This layer comprises the resistor terminations, acts as a "reinforcement" for the solder pads and also as the "top" conductor for the crossovers.

The use of the commercial ESL 3114 resistor was preferred to our model V6-based resistors; although both feature good strain-sensing performance and stability [23][36][51]; commercial compositions tend to have more reproducible properties, and, especially, feature additives to compensate their temperature coefficient of resistance (TCR).

Overglaze

Finally, a protective layer of straight V8 glass was deposited and fired at 450°C, ending the "high-temperature" processing steps.

---

1 Alfa Aesar, α-Al_2O_3, 99.99%, ≈ 1 µm particle size.

2 Alfa Aesar Fe_2O_3 014680, 99.945%, <5 µm.

3 Quarzwerke, Sikron cristobalite flour SF8000, ≈2.5 µm particle size (D50).

4 Nanostructured & Amorphous Materials Inc., SiO_2 99.95%, ≈2.5…3 µm particle size (D50).

5 Nanostrutured & Amorphous Materials Inc., Ag 99.9%, APS 30 nm

2.5. Comparison with the "standard" materials system

A comparison of the new thick-film system vs. the commercial-based older "standard" system used for the first sensor version is given in Table 3. This older system, based on commercial materials, requires a standard thick-film firing temperature of 850°C, which poses materials compatibility issues and increases thermal mismatch stresses. Fabrication of reliable crossovers using this system was not possible with any of the commercial dielectrics in Table 3, leading to the aforementioned spalling problems (section 1.2), and a custom solution with a lower stress had to be introduced.

Compared to this previous system, the low-firing one developed in our studies features compatibility with a much wider range of steels, especially high-strength martensitic ones, and in general much lower thermal exposure of the substrate, hinting at possible application, with further refinements, to titanium or even some aluminium alloys.

A photograph of the resulting device is given in Figure 8.

Layer (# prints)	**Low-firing system**	**"Standard" system**
Overglaze	V8 (450°C)	V8 + 20% Al_2O_3 (465°C)
Top conductor	Ag + 10% V8 (500°C)	ESL 590G (465°C)
Crossover dielectric	(= main)	V8 + 40% Al_2O_3 (525°C)
Resistor (termination)	ESL 3114 (top)	DuPont 2041 (bottom)
Bottom conductor	ESL 9912 (Ag)	ESL 9635B (AgPd)
Compatibility diel.	V6 + Al_2O_3	ESL 4924 or Heraeus GPA 98-029
Main dielectric	V6 + SiO_2 (quartz or cristobalite)	
Adhesion dielectric	V6 + Fe_2O_3	ESL 4916

Table 3. Comparison of old & new thick-film systems. Firing temperature is 625°C peak for the low-firing and 850°C for the "standard" system, unless indicated otherwise.

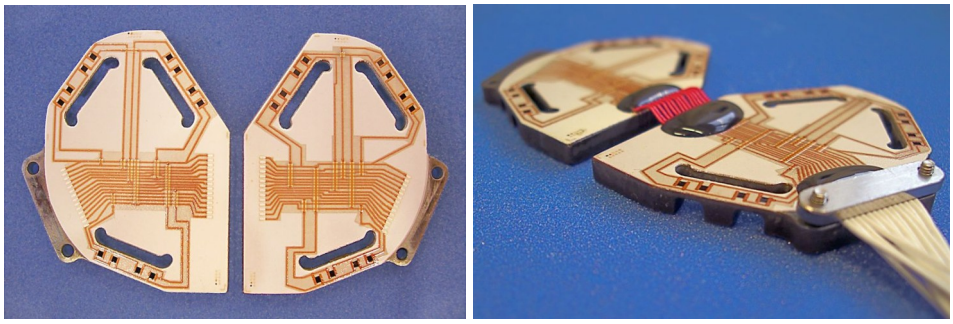

Figure 8: Thick-film piezoresistive sensor with low-firing materials system.

3. Fabrication of the force sensor

3.1. Mechanical structure

The developed force-sensing device [1][4][5][6] (Figure 3) consists of two sensitive plates, one for each condyle, and a tibial base plate, which is fixed by customised surgical pins. The device is placed in the tibio-femoral gap in place of the ultimate prosthesis (Figure 4). Each sensitive plate, designed for a maximal load of 500 N, contains three deformable bridges, which are instrumented with thick-film piezoresistive sensors (Figure 9). Applying a load in the sensitive area generates three vertical reaction forces (Figure 10), one in each bridge, measured by the corresponding sensors. The three measured forces then allow determination of the amplitude and location of the applied load for each condyle, from which the net varus-valgus ligamentous moment and force imbalances may be computed, help the surgeon to balance the joint [1][4].

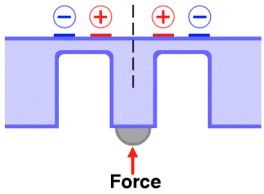

Figure 9. Schematic instrumentation of each deformable bridge with piezoresistors.

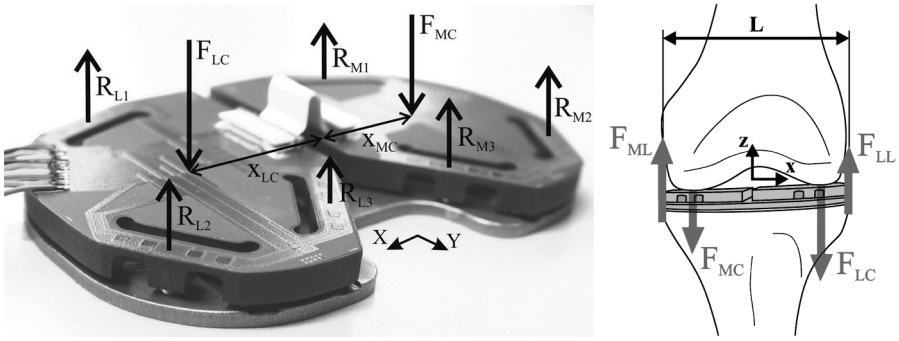

Figure 10: Contact forces *F* and reaction forces *R* of the bridges (left), and depiction in the joint (right) [4].

In static conditions, for one plate, the mechanic equilibrium equations are [4]:

$$\sum_i \vec{F}_i = \vec{0} \text{ and } \sum_i \vec{M}_i = \vec{0} \qquad (2)$$

Hence:

$$F = R_1 + R_2 + R_3\,,\; x = \frac{x_1R_1 + x_2R_2 + x_3R_3}{R_1 + R_2 + R_3} \text{ and } y = \frac{y_1R_1 + y_2R_2 + y_3R_3}{R_1 + R_2 + R_3} \qquad (3)$$

where F is the applied force, R_i the reaction forces at the bridges, (x,y) the position of the application point of F, and (x_i,y_i) the positions of the bridge supports, which consist of 3 mm diameter bearing steel balls seated in the bridge central pillars (see Figure 9), contacting on a titanium baseplate [1].

The sensor plates were machined out of the same Sandvik Bioline High-N austenitic steel [17], as in the original version.

3.2. Layout & thick-film deposition

The layout of electrical circuit is depicted on Figure 11 (see Figure 3 for actual size). The layout is similar to that of the previous version, but adapted to the new materials system, to include the resistor terminations in the top conductor (section 2).

Here, "dielectrics 1-3" are the layouts for the adhesion (1), main / compatibility (2) and crossover (3) dielectrics (Figure 7, Table 2 & Table 3). "Silvers 1-2" are the bottom and top conductor, and "glass" denotes the overglaze layer. The layout for the main and compatibility dielectric are identical, while that for the adhesion is slightly (ca. 0.15 mm) enlarged in all directions to avoid spalling on the sides. The piezoresistors ("resistor") for each force-sensing bridge are arranged in accordance with Figure 9. The thick-film sequence was deposited using the new materials system described in section 2, using the variant for austenitic steels.

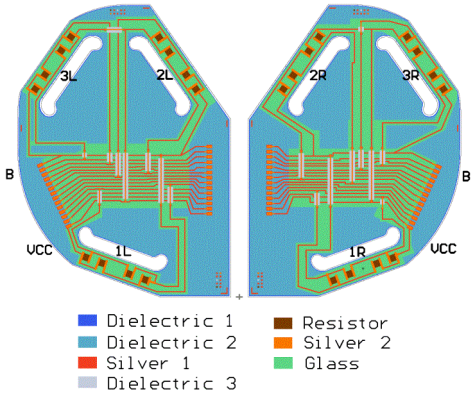

Figure 11. Layout of the sensor, with the overglaze drawn below some layers for better visibility.

3.3. Interconnections and protection

After the thick-film part, Teflon-insulated cables were soldered (Sn-Ag-Cu solder) on the thick-film Ag contact pads, and the mechanical stability of this assembly was improved by dispensing epoxy resin (Emerson & Cuming, Stycast 2651MM + catalyst 24LV, 100:13 parts by weight) onto the resulting contacts.

Finally, as the use of lead-based glassy materials poses some concern for surgical instruments, constituting a (limited) risk of leaching into the patient, the sensor was conformally covered with a parylene C coating (ca. 10 µm).

4. Characterisation of the new sensor

4.1. Setup and experiments

Each plate left (L) and right (R) is calibrated independently. Using calibrated weights, we applied a force from 0 to 100 N on 4 points on each plate of the sensor as depicted on Figure 12 – the point coordinates being given in Table 4 – using the setup [1][4] depicted in Figure 13. The output signals are measured with a specific set of amplifiers and collected using a computer calibration interface (Figure 14).

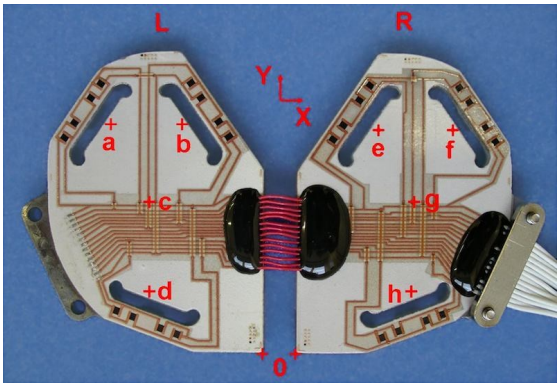

Figure 12: Calibration points

Point	***x*** [mm]	***y*** [mm]
a	-26	31
b	-14	31
c	-20	21
d	-20	11
e	14	31
f	28	31
g	20	21
h	20	6

Table 4: Position of the calibration points.

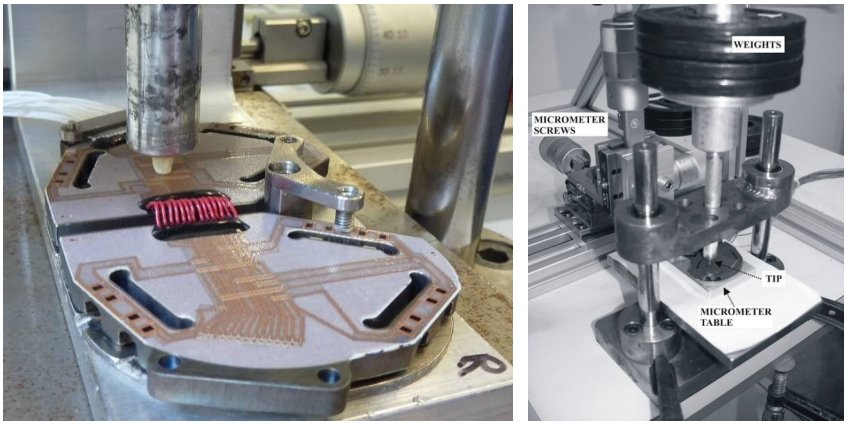

Figure 13: Measurement setup

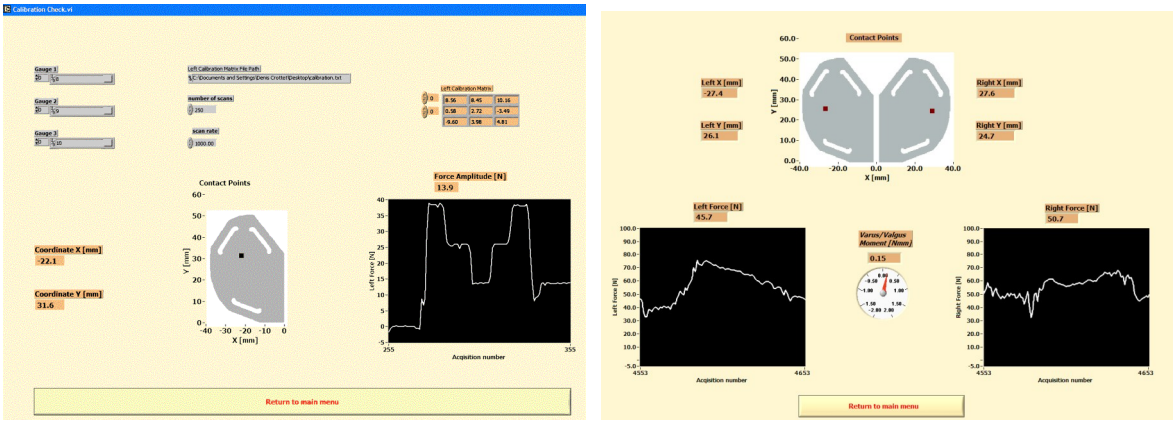

Figure 14. Screenshot of the calibration & acquisition software [1] (left) & measurement pane (right).

4.2. Data analysis

For each force on one plate, we obtain three signals $S_{1\ldots3}$ from the three reaction forces of the bridges (see Figure 10). According to (3), the applied force F can therefore be written as a linear combination of these 3 signals and the calibration factors $u_{1\ldots3}$:

$$F = u_1 \cdot S_1 + u_2 \cdot S_2 + u_3 \cdot S_3 \tag{4}$$

Likewise, the moments in X and Y are given by:

$$M_x = F \cdot x = u_1 \cdot x_1 \cdot S_1 + u_2 \cdot x_2 \cdot S_2 + u_3 \cdot x_3 \cdot S_3 \tag{5}$$

$$M_y = F \cdot y = u_1 \cdot y_1 \cdot S_1 + u_2 \cdot y_2 \cdot S_2 + u_3 \cdot y_3 \cdot S_3 \tag{6}$$

For each measurement, we know F, x, y (applied), and S_i (measured, $i = 1\ldots3$). First, according to (4), multiple linear regression analysis of F vs. S_i directly gives the calibration factors u_i. The same procedure, carried out on $F{\cdot}x$ vs. $x_i{\cdot}S_i$ and $F{\cdot}y$ vs. $y_i{\cdot}S_i$ yields, following (5) and (6), the coefficients $(u_i{\cdot}x_i)$ and $(u_i{\cdot}y_i)$ respectively. Dividing those by the previously obtained u_i allows us to extract the positions (x_i,y_i) of the application points of the reaction forces, which can be compared for consistency with the mechanical drawings.

4.3. Results and discussions

The results are shown here in Figure 15, Figure 16 & Figure 17 for the right force-sensing plate, separated in four curves according to the force application point e-h, with connecting lines between points being only guides for the eye. Errors are calculated as the difference between the values calculated from the regression parameters and those derived from the applied force and positions.

Figure 15 shows the results for the total force. All errors lie within a ±1.5 N band, with a transition clearly evident between zero and the first applied force (0…14 N), which may be due to parasitic forces arising from friction between the steel balls and the supporting plate. Also, limited friction (< 1 N) is present in the force-application device, which also contributes to apparent errors.

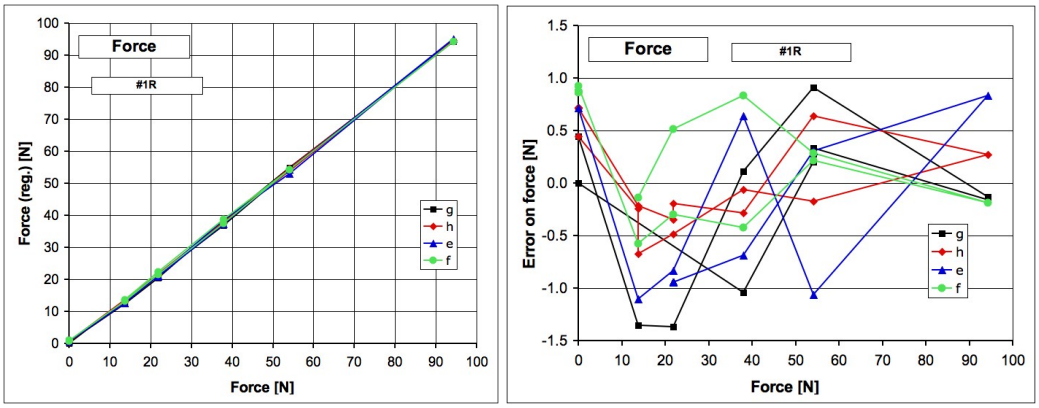

Figure 15: Force from signal & coefficients (left) and error (right) vs. applied force
(force application points e-h: see Figure 12 & Table 4).

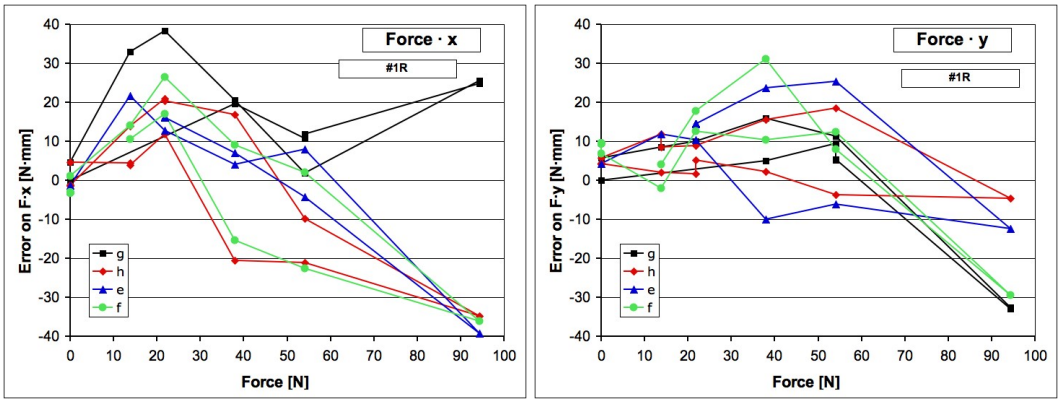

Figure 16: Errors on moments *F·x* (left) and *F·y* (right) vs. applied force
(force application points e-h: see Figure 12 & Table 4).

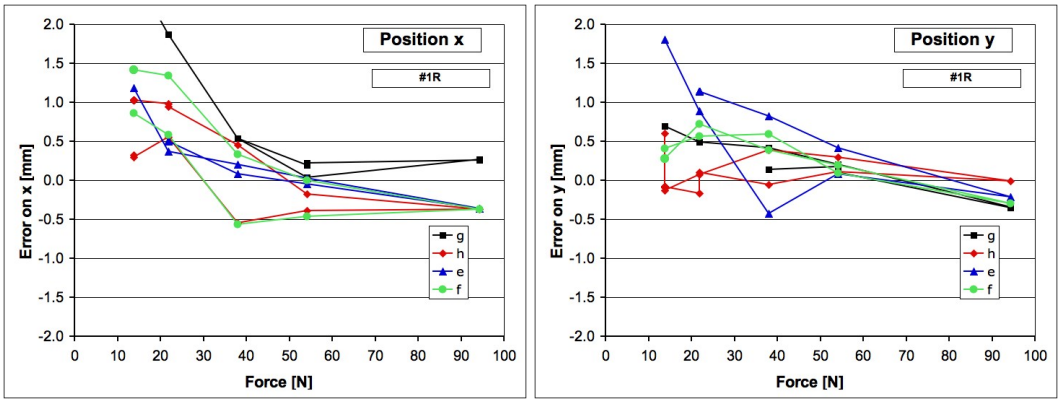

Figure 17: Errors on positions *x* and *y* vs. applied force
(force application points e-h: see Figure 12 & Table 4).

Figure 16 & Figure 17 show the results for the moments and positions in X and Y. The error on position becomes less than 1 mm above ≈30 N, which is good given the fact that the force application point is not very precise, given the relatively large 2 mm diameter and polymer cushion of the force application pin, needed to avoid damage to the thick-film circuit. This may also contribute to the small but significant discrepancy (< 1 mm) between the position of the bridges derived from regression analysis and their actual position in the mechanical drawings.

Another potential source of error comes from the thick-film bridges themselves, the experimental device having poor homogeneity between the resistor values due to variations in screen-printing thicknesses. While this does not prevent the device from working, it does make each force-sensing bridge more sensitive to parasitic loads such as caused by lateral friction of the balls on the support. In contrast, these loads essentially cancel out in an ideally symmetrical bridge with perfectly identical resistors. A final error contribution may also come from the main dielectric of the low-firing thick-film system itself, especially the one for austenitic steels used in this device. Both dielectric variants (ferritic/martensitic or austenitic) use SiO_2 fillers that exhibit a displacive phase transition, lying nominally at 573°C for quartz and 260°C for cristobalite [42]. Especially the latter transformation could be reversed by the presence of large stresses, constituting a potential source of mechanical hysteresis. Previous studies on pressure sensors machined out of austenitic and ferritic steels and the associated thick-film systems [25] indeed show larger apparent drifts with the low-firing systems compared to the commercial one. Nevertheless, the performance is acceptable for medical devices, where instrumentation-grade precision is not necessary given the large natural variation in physiological parameters.

5. Conclusion & outlook

5.1. Achievements

In the frame of the NCCR CO-ME project (II-6), we have developed a range of low-firing thick-film material systems for steel, which allow fabrication of load sensors on ferritic, martensitic and austenitic steels, and even, experimentally, on aluminium alloys. For steel, we developed a "standard" system firing at 625°C, with two variants (one for ferritic & martensitic and the other for austenitic steels) differing by only one layer, the main dielectric, for optimal thermal expansion matching to the substrate.

These developed materials were extensively characterised in numerous studies focused on their structural evolution and properties, with the aim of obtaining working and reliable systems. After this necessary step, demonstration was made of their piezoresistive load sensing properties, first with pressure sensor test structures and finally with the previously developed TKA force sensor structure. These tests demonstrated that low-firing materials could achieve a level of performance sufficient for application to the field of medical instruments.

Compared to standard commercial thick-film materials systems such as the one used to first instrument the TKA sensor, the lower 625°C firing temperature considerably improves the compatibility of the thick-film process with metallic alloys, drastically reducing problems associated with oxidation and annealing effects and altogether avoiding the phase transition issues that had hitherto precluded the use of thick-film technology on the common and very favourable high-strength martensitic alloys.

5.2. Outlook

Although sensing surfaces in medical instruments may be covered by parylene or any other packaging method to minimise their interaction with the human body, the ubiquitous presence of lead – or even small amounts of cadmium in the used commercial resistor compositions – still poses a concern, and would be very problematic for a possible extension to long-term implants. Therefore, the most important future challenge is to remove lead in the system by introducing suitable equivalent low-melting glasses - although no exact substitute is known to exist to the lead borosilicate system.

First tests with SnO-ZnO-P_2O_5 phosphate glasses were unsuccessful. Although promising, these glasses have a radically different (reducing) chemistry, and would need considerable development effort to rebuild a new thick-film system. Therefore, we decided – with more success to focus our efforts on bismuth borate glasses, more exactly on the Bi_2O_3-B_2O_3-ZnO-SiO_2-Al_2O_3 oxide system with optional further additives, which are known to have properties that are reasonably close to that of lead borosilicate compositions, Bi_2O_3 having some similarity with PbO [53].

We therefore formulated and studied a series of bismuth glasses, applying them in a similar manner as the V6 and V8 lead borosilicate frits to formulate a series of conductive, dielectric, piezoresistive and overglaze compositions. Our first results for resistors [28][29], which are depicted in, are very promising, achieving the desired sheet resistance in the ≈10 kΩ range and moderate TCR values even without additives. We were also able de qualitatively verify that our resistors indeed exhibit piezoresistive response, which was also independently observed by another team developing similar compositions [54].

Finally, the low achieved resistor firing temperatures, down to ca. 525°C, clearly demonstrate the application potential of these materials to the manufacture of thick-film piezoresistive sensors on steel substrates. Furthermore, these results lead us to envision fabrication of thick-film sensors or other electronic circuits on other substrates such as glass and some aluminium alloys.

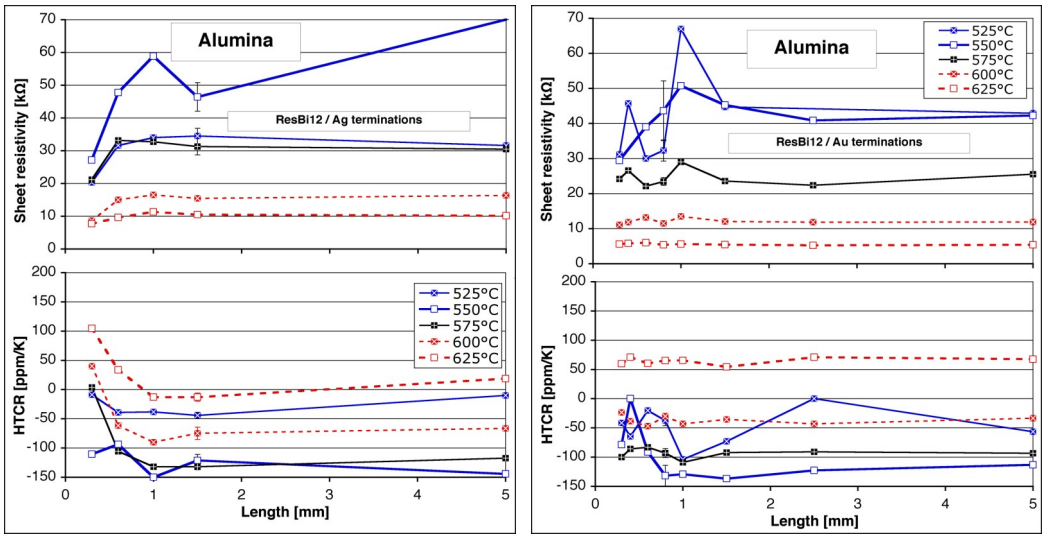

Figure 18: Sheet resistance at 25°C and its temperature coefficient (HTCR, 25-100°C) vs. resistor length and firing temperature (the lines are only guides to the eye).

6. Bibliography

[1] Crottet-D, "A force-sensing device for assistance in soft-tissue balancing during knee arthroplasty", thesis no 3398, EPFL, Switzerland, 2005.

[2] Fehring-TK Valadie-AL, "Knee instability after total knee arthoplasty", Clinical Orthopaedics and Related Research 299, 157–162, 1994.

[3] Moreland-JR, "Mechanisms of failure in total knee arthroplasty", Clinical Orthopaedics and Related Research 226, 49–64, 1988.

[4] Crottet-D Maeder-T Fritschy-D Bleuler-H Nolte-LP Pappas-IP, "Development of a force amplitude- and location-sensing device designed to improve the ligament balancing procedure in TKA", IEEE Transactions on Biomedical Engineering Vol. 52 (9), 1609-1611, 2005.

[5] Crottet-D Maeder-T Sarfert-SA Fritschy-D Bleuler-H Nolte-LP Pappas-IP, "In-vitro evaluation of a force-sensing device for ligament balancing in TKA", 51st Annual Meeting of the Meeting of the Orthopaedic Research Society, Washington (USA), 2005.

[6] Crottet-D Kowal-J Sarfert-SA Maeder-T Bleuler-H Nolte-LP Dürselen-L, "Ligament balancing in TKA: Evaluation of a force-sensing device and the influence of patellar eversion and ligament release", Journal of Biomechanics Vol. 40 (8), 1709-1705, 2007.

[7] Crottet-D Pappas-IP Maeder-T Jacq-C Bleuler-H, "A force-sensing device for ligament balancing in total knee arthroplasty", International Patent WO 2005/122899, 2005.

[8] Plus Orthopaedics, San Diego, USA [now a division of Smith & Nephew, UK], 2005.

[9] Morten-B Prudenziati-M, "Piezoresistive thick-film sensors", Handbook of Sensors and Actuators vol. 1: Thick film sensors / ed. by M. Prudenziati, Elsevier, 189-208, 1994.

[10] Wada-T Stein-SJ Stein-MA Chitale-SM, "The state-of-the-art of thick film technology for automotive sensors", Proceedings, IEMT/IMC Symposium, 41-46, 1997.

[11] White-NM Turner-JD, "Thick-film sensors: past, present and future", Measurement Science and Technology Vol. 8, 1-20, 1997.

[12] White-NM Turner-JD, "Thick-film sensors: past, present and future", Proceedings, 14th International Conference on Solid-State Sensors, Actuators and Microsystems - Transducers / Eurosensors'07, Lyon, France, 107-111, 2007.

[13] Maeder-T Jacq-C Birol-H Ryser-P, "High-strength ceramic substrates for thick-film sensor applications", Proceedings, 14th European Microelectronics and Packaging Conference - IMAPS, Friedrichshafen (DE), 133-137, 2003.

[14] Maeder-T Birol-H Jacq-C Ryser-P, "Strength of ceramic substrates for piezoresistive thick-film sensor applications", Proceedings, European Microelectronics and Packaging Symposium, Prague (CZ), 272-276, 2004.

[15] Maeder-T Jacq-C Corradini-G Ryser-P, "Effect of thick-film materials on the mechanical integrity of high-strength ceramic substrates", Proceedings of the 15th European Microelectronics and Packaging Conference (EMPC), Brugge (BE), IMAPS, S16.03, 377-381, 2005.

[16] Jacq-C Maeder-T Ryser-P, "High-strain response of piezoresistive thick-film resistors on titanium alloy substrates", Journal of the European Ceramic Society Vol. 24 (6), 1897-1900, 2004.

[17] "Sandvik Bioline® - Advanced materials for medical and dental products", Sandvik AB, Sandviken, Sweden, www.sandvik.com/bioline, 2002.

[18] Jacq-C Vionnet-S Maeder-T Ryser-P, "Integrated thick-film hybrid microelectronics on aluminium substrates", Proceedings, European Microelectronics and Packaging Symposium, Prague (CZ), 267-271, 2004.

[19] Jacq-C Maeder-T Vionnet-S Ryser-P, "Low-temperature thick-film dielectrics and resistors for metal substrates", Journal of the European Ceramic Society Vol. 25 (12), 2121-2124, 2005.

[20] Jacq-C Maeder-T Menot-Vionnet-S Birol-H Saglini-I Ryser-P, "Integrated thick-film hybrid microelectronics applied on different material substrates", Proceedings of the 15th European Microelectronics and Packaging Conference (EMPC), Brugge (BE), IMAPS, S13.04, 319-324, 2005.

[21] Jacq-C Maeder-T Vionnet-Menot-S Grimaldi-C Saglini-I Ryser-P Carreño-Morelli-E, "Development of low-temperature thick-film materials for piezoresistive sensors", Proceedings, Sintering'05, Grenoble (FR), 3b1, 200-203, 2005.

[22] Hrovat-M Maeder-T Jacq-C Holc-J Bernard-J, "Subsolidus phase equilibria in the PbO-poor part of the TiO_2–PbO–SiO_2 system and its application in low-temperature thick-film dielectrics", Journal of Materials Research Vol. 21 (12), 3210-3214, 2006.

[23] Vionnet-Menot-S Maeder-T Grimaldi-C Jacq-C Ryser-P, "Properties and stability of thick-film resistors with low processing temperatures - effect of composition and processing parameters", Journal of Microelectronics and Electronic Packaging Vol. 3 (1), 37-43, 2006.

[24] Jacq-C Maeder-T Johner-N Corradini-G Ryser-P, "High performance low-firing temperature thick-film pressure sensors on steel", Proceedings, 16th IMAPS European Microelectronics & Packaging Conference (EMPC), Oulu, Finnland, 167-170, 2007.

[25] Jacq-C Maeder-T Ryser-P, "Piezoresistive properties of low-firing temperature thick-films on steel sensors", Proceedings, International Conference on Ceramic Interconnect and Ceramic Microsystems Technologies (CICMT), Munich (DE), 411-416 (P13), 2008.

[26] Jacq-C Maeder-T Ryser-P, "Load sensing surgical instruments", Journal of Materials Science: Materials in Medecine, 2008.

[27] Prudenziati-M Morten-B Moro-L Olumekor-L Tombesi-A, "Interactions between thick-film resistors and terminations: the role of bismuth", Journal of Physics D: Applied Physics Vol. 19, 275-282, 1986.

[28] Maeder-T Jacq-C Grimaldi-C Ryser-P, "Lead-free low-firing thick-film resistors based on bismuth glasses and ruthenium oxide", Proceedings, XXXIII International Conference of IMAPS Poland Chapter, Gliwice – Pszczyna, Poland, 222-229, 2009.

[29] Jacq-C Maeder-T Ryser-P, "Development of low-firing lead-free thick-film materials on steel alloys for piezoresistive sensor applications", Proceedings, 17th IMAPS European Microelectronics & Packaging Conference (EMPC), Rimini, Italy, P07, 2009.

[30] Bilinski-M Eisermann-E Jones-Williams-K Smetana-W Unger-M Whitmarsh-J, "Thick film pastes for the manufacture of low cost, insulated aluminium substrates for use as integrated heat sinks for high intensity LEDs", Proceedings, XXXII International Conference of IMAPS Poland Chapter, Pułtusk, Poland, I12, 2008.

[31] Hoffman-LC, "Crystallizable dielectrics in multilayer structures for hybrid microcircuits: a review", Ceramic Substrates and Packages for Electronic Applications (Advances in Ceramics vol 26) Vol. 26, 249-253, 1989.

[32] Grimaldi-C Vionnet-Menot-S Maeder-T Ryser-P, "Effect of composition and microstructure on the transport and piezoresistive properties of thick-film resistors", Proceedings, XXVIII International Conference of IMAPS Poland Chapter, Wroclaw, 35-42, 2004.

[33] Vionnet-S Grimaldi-C Ryser-P Maeder-T Strässler-S, "Strain modulation of transport criticality in RuO_2-based thick-film resistors", Applied Physics Letters Vol. 85 (23), 5619-5621, 2004.

[34] Vionnet-Menot-S, "Low firing temperature thick-film piezoresistive composites - properties and conduction mechanism", thesis no 3290, EPFL, Switzerland, 2005.

[35] Vionnet-Menot-S Grimaldi-C Maeder-T Ryser-P Strässler-S, "Study of electrical properties of piezoresistive pastes and determination of the electrical transport ", Journal of the European Ceramic Society Vol. 25 (12), 2129-2132, 2005.

[36] Vionnet-Menot-S Grimaldi-C Maeder-T Ryser-P Strässler-S, "Tunneling-percolation origin of nonuniversality: Theory and experiments", Physical Review B Vol. 71, 064201, 2005.

[37] Johnson-DW Hummel-FA, "Phase equilibria and liquid immiscibility in the system PbO-B_2O_3-SiO_2", Journal of the American Ceramic Society Vol. 51 (4), 196-201, 1968.

[38] Trubnikov-IL, "Thermal expansion and corrosion behavior of lead-borosilicate glasses", Refractories and Industrial Ceramics Vol. 41 (5-6), 169-171, 2000.

[39] Prudenziati-M Morten-B Forti-B Gualtieri-AF Dilliway-GM, "Devitrification kinetics of high lead glass for hybrid microelectronics", International Journal of Inorganic Materials Vol. 3, 667-674, 2001.

[40] Ram-S Narayan-KA, "Controlled crystallization of PbO-Cr_2O_3-B_2O_3 glasses and a catalytic effect of Al_2O_3 for the growth of Pb_2CrO_5 microcrystals", Industrial & Engineering Chemistry Research Vol. 26, 1051-1055, 1987.

[41] Ram-S Ram-K Shukla-BS, "Optical absorption and EPR studies of borate glasses with $PbCrO_4$ and Pb_2CrO_5 microcrystals", Journal of Materials Science Vol. 27, 511-519, 1992.

[42] Taylor-D, "Thermal expansion data 4. Binary oxides with the silica structures", British Ceramic: Transactions and Journal Vol. 83 (5), 129-134, 1984.

[43] "3100 series", product catalogue & materials safety data sheet no. 415, ElectroScience Laboratories (ESL), King of Prussia, USA, www.electroscience.com, 2007.

[44] Storbeck-I Wolf-M, "About the influence of SiO_2 on the temperature behaviour of ruthenate based thick film resistors", Active and Passive Electronic Components Vol. 12 (3), 149-153, 1987.

[45] Monneraye-M, "Les encres sérigraphiables en microélectronique hybride: les matériaux et leur comportement [Screenable inks in hybrid microelectronics: the materials and their behaviour]", Acta Electronica Vol. 21 (4), 263-281, 1978.

[46] Hoffman-LC, "Crystallizable dielectrics in multilayer structures for hybrid microcircuits: a review", Ceramic Substrates and Packages for Electronic Applications (Advances in Ceramics vol 26) Vol. 26, 249-253, 1989.

[47] Pavlushkin-NM Zhuravlev-AK Egorova-LS, "Change in the phase compositions of lead glasses during crystallization", Inorganic materials Vol. 4, 403, 1968.

[48] Tummala-RR, "Low-temperature and low-expansion glass-crystal composites by the formation of Perovskite lead titanate", Journal of Materials Science Vol. 11, 125-128, 1976.

[49] Taylor-D, "Thermal expansion data 8. Complex oxides, ABO_3, the perovskites", British Ceramic : Transactions and Journal Vol. 84 (6), 181-188, 1985.

[50] Taylor-D, "Thermal expansion data 10. Complex oxides, ABO_4", British Ceramic : Transactions and Journal Vol. 85 (5), 147-155, 1986.

[51] Vionnet-S Maeder-T Ryser-P, "Firing, quenching and annealing studies on thick-film resistors", Journal of the European Ceramic Society Vol. 24 (6), 1889-1892, 2004.

[52] Inokuma-T Taketa-Y, "Control of electrical properties of RuO_2 thick film resistors", Active and Passive Electronic Components Vol. 12, 155-166, 1987.

[53] Heynes-MSR Rawson-H, "Bismuth trioxide glasses", Journal of the Society of Glass Technology 41, 347-349, 1957.

[54] Totokawa-M Yamashita-S Morikawa-K Mitsuoka-Y Tani-T Makino-H, "Microanalyses on the RuO_2 particle–glass matrix interface in thick-film resistors with piezoresistive effects", International Journal of Applied Ceramic Technology Vol. 6 (2), 195-204, 2009.